













The Vera C. Rubin Observatory Data Preview 2

VERA C. RUBIN OBSERVATORY TEAM,¹ ERIC C. BELLM ², LEANNE P. GUY ³, MINHEE HYUN ⁴, YIJUNG KANG ^{5,3},
ARUN KANNAWADI ^{6,7}, KSHITJA KELKAR ³, SHUANG LIANG,⁸ KIAN-TAT LIM ⁸, JAMES R. MULLANEY ⁹,
KATE NAPIER ⁵, WILLIAM O’MULLANE ³, AASHAY PAI ¹⁰ AND IAN S. SULLIVAN ²

¹NSF-DOE Vera C. Rubin Observatory / NSF NOIRLab, 950 N. Cherry Ave., Tucson, AZ 85719, USA

²University of Washington, Dept. of Astronomy, Box 351580, Seattle, WA 98195, USA

³NSF-DOE Vera C. Rubin Observatory / NSF NOIRLab, Casilla 603, La Serena, Chile

⁴Stanford University, 450 Jane Stanford Way, Stanford, CA 94305, USA

⁵Kavli Institute for Particle Astrophysics and Cosmology, SLAC National Accelerator Laboratory, 2575 Sand Hill Rd., Menlo Park, CA 94025, USA

⁶Department of Physics, Duke University, Durham, NC 27708, USA

⁷Department of Astrophysical Sciences, Princeton University, Princeton, NJ 08544, USA

⁸SLAC National Accelerator Laboratory, 2575 Sand Hill Rd., Menlo Park, CA 94025, USA

⁹Astrophysics Research Cluster, School of Mathematical and Physical Sciences, University of Sheffield, Sheffield, S3 7RH, United Kingdom

¹⁰Department of Astronomy and Astrophysics, University of Chicago, 5640 South Ellis Avenue, Chicago, IL 60637, USA

(Dated: June 22, 2026)

ABSTRACT

We present Rubin Data Preview 2 (DP2), the second data preview from the NSF-DOE Vera C. Rubin Observatory,

Keywords: Rubin Observatory - LSST

1. INTRODUCTION

2. COMMISSIONING WITH LSSTCAM

3. OVERVIEW OF THE CONTENTS OF RUBIN DP2

4. DATA RELEASE PROCESSING

Data Release Processing (DRP) is the data pipeline that produces the calibrated images, detection catalogs, and derived data products defined in section §TBD, using the LSST Science Pipelines (citation). DP2 was processed at the United States Data Facility (USDF) at SLAC, with pilot runs at the National Institute of Nuclear and Particle Physics (IN2P3) computing center.

The processing campaign consists of four major stages: (1) single-frame processing, (2) calibration, (3) multi-visit processing, (4) variable and transient source processing. Data quality and key metrics for verification and validation are actively monitored during each stage, and comprehensive verification and validation assessments are completed before processing the next stage.

This section describes the high-level algorithms, configurations, and verification metrics for each stage, including changes and improvements from DP1 (citation).

4.1. Single-Visit Processing

4.1.1. Calibration & Instrument Signature Removal (ISR)

4.1.2. Background Subtraction

`CalibrateImageTask` is the pipeline task responsible for PSF characterization, astrometric and photometric calibration, and source detection on individual exposures. As part of this processing, it models and removes the large-scale sky background prior to source measurement and downstream multi-visit data processing. Applied after ISR has removed instrumental signatures, this step is designed to preserve astrophysical structure on source scales while suppressing broad background structure that would otherwise bias detection thresholds, photometry, and deblending.

An initial background model (`psf_subtract_background`) is subtracted prior to PSF characterization and preliminary source detection. The background is estimated by dividing the image into 128×128 pixel superpixels and computing the iterative 3σ -clipped mean of unmasked pixels in each bin. Pixels flagged as BAD, EDGE, DETECTED, DETECTED_NEGATIVE, or NO_DATA are

Corresponding author: Leanne P. Guy

63 excluded. The resulting coarse map is modeled with
 64 a sixth-order two-dimensional Chebyshev polynomial,
 65 which is evaluated at native pixel resolution via Akima
 66 spline interpolation.

67 After PSF fitting, aperture correction, and astrometric
 68 calibration, this first-pass model is discarded and the
 69 background is restored onto the image to allow for the
 70 second estimate to be fit on the full sky signal. By this
 71 stage the DETECTED mask plane has been updated by
 72 PSF-stage source detection, providing a more complete
 73 and accurate source mask than was available for the
 74 initial estimate. Before fitting the second background
 75 model, these mask planes are further dilated by up to
 76 10 pixels to suppress source-wing flux from leaking into
 77 the background bins.¹¹ The dilation is iteratively re-
 78 duced by 1 pixel at a time if it would mask more than
 79 93% of unmasked pixels. The dilated mask planes are
 80 used only for the background estimation and are cleared
 81 before the final source-detection pass.

82 A second background estimate (`star_background`) is
 83 then computed on the updated source-masked image
 84 and subtracted before the final source-detection pass.
 85 The algorithm configuration is identical to `psf_sub-`
 86 `tract_background`: 128×128 pixel superpixels, MEAN-
 87 CLIP statistics, a sixth-order Chebyshev polynomial,
 88 and Akima spline interpolation.

89 Finally, following the `star_background` fit, a zeroth-
 90 order pedestal correction is applied to account for any
 91 large-scale oversubtraction introduced by the higher-
 92 order model. This can occur particularly in crowded
 93 fields where many pixels are covered by source flux.¹²
 94 The pedestal is a constant offset measured from the
 95 `star_background`-subtracted image. It is measured
 96 iteratively over increasing bin sizes, starting at $32 \times$
 97 32 pixels for a full LSSTCam detector and doubling each
 98 iteration. At each step a new constant offset is fit
 99 and subtracted. Iteration continues until the cumula-
 100 tive pedestal level changes by less than 5% relative to
 101 the previous step, or by less than 0.5 counts in abso-
 102 lute terms, indicating that the estimate has stabilized
 103 across spatial scales. The `star_background` model and
 104 all pedestal corrections together constitute the output
 105 background model (`preliminary_visit_image_back-`
 106 `ground`; see Figure 1).

107 Compared to DP1 (?), several changes were made
 108 to the background subtraction for DP2. The in-
 109 line background re-estimation that DP1 performed
 110 after each detection pass (`reEstimateBackground =`
 111 `True`) has been replaced by the dedicated `star_-`
 112 `background` subtask, which re-estimates the full back-
 113 ground model from scratch with a more complete
 114 source mask. This change is enabled by the introduc-
 115 tion of adaptive threshold detection (`do_adaptive_-`
 116 `threshold_detection = True`), which iteratively ad-
 117 justs the detection threshold to ensure the source mask
 118 used for `star_background` is neither too sparse nor
 119 too aggressive. The mask dilation and pedestal cor-
 120 rection described above are also new in DP2, as is
 121 diffraction spike masking (`doMaskDiffractionSpikes`
 122 `= True`), which adds a SPIKE mask plane prior to back-
 123 ground estimation. Finally, the per-step illumination
 124 correction that DP1 applied during background esti-
 125 mation (`doApplyFlatBackgroundRatio = True`, `do_-`
 126 `illumination_correction = True`) has been disabled.
 127 These corrections are now handled upstream in ISR
 128 rather than within the background model itself.

129 Following background subtraction, `CalibrateImage-`
 130 `Task` computes several statistics on the residual image
 131 and stores them in the task metadata. The median and
 132 standard deviation of all unmasked pixels are recorded,
 133 as are the median and standard deviation of fluxes mea-
 134 sured on *sky sources*, which are empty apertures placed
 135 in source-free regions of the image. The sky source
 136 statistics are a particularly direct probe of background
 137 subtraction quality, as any residual signal in these aper-
 138 tures is attributable to background model error rather
 139 than astrophysical flux.

¹¹ When fewer than 50% of pixels are detected, an additional 2-pixel dilation is applied to the DETECTED mask before the pedestal fit, to further suppress source contamination in sparsely detected regions.

¹² During pedestal fitting, pixels flagged as SAT, SUSPECT, or SPIKE are additionally excluded, beyond the standard `SubtractBackgroundTask` ignored pixel mask.

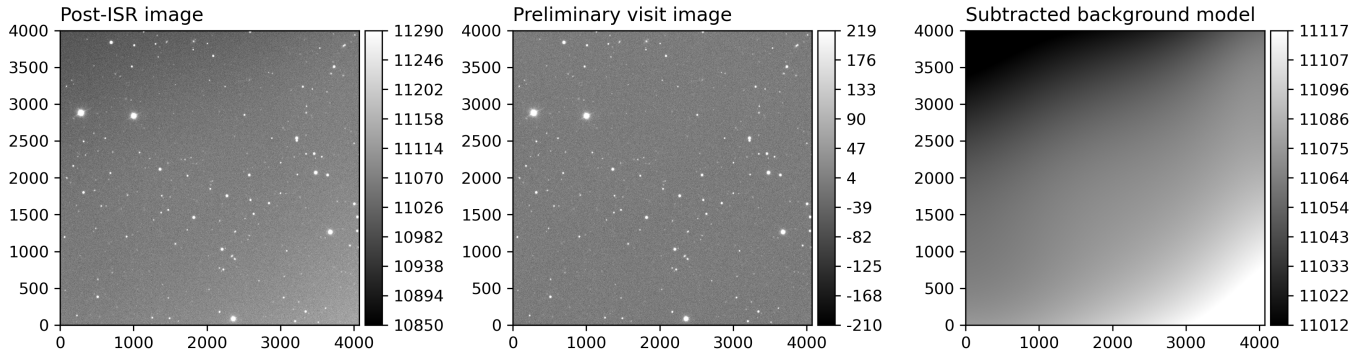


Figure 1. Background subtraction for LSSTCam visit 2025110500300, detector 25. *Left:* Post-ISR image (`post_isr_image`), before any background removal. *Center:* Preliminary visit image (`preliminary_visit_image`), after background subtraction by `CalibrateImageTask`. *Right:* The subtracted background model (`preliminary_visit_image_background`), illustrating the large-scale structure removed. All three panels use a linear stretch clipped to the central 95th percentile of pixel values.

4.2. Calibration

4.2.1. PSF Modeling

4.2.2. Astrometric Calibration

4.2.3. Photometric Calibration

4.3. Multi-Visit Processing

4.3.1. Input Data Selection

4.3.2. Coaddition

4.3.3. Detection, Deblending, & Measurement

4.3.4. First Look

4.4. Variable & Transient Source Processing

4.4.1. Light Curves

4.4.2. Solar System Processing

4.4.3. Difference Image Analysis (DIA)

4.4.4. Artifact Rejection

5. PERFORMANCE CHARACTERIZATION AND KNOWN ISSUES

6. RUBIN SCIENCE PLATFORM

7. SUPPORT FOR COMMUNITY SCIENCE

8. SUMMARY AND FUTURE RELEASES

ACKNOWLEDGMENTS

. This material is based upon work supported in part by the National Science Foundation through Cooperative Agreements AST-1258333 and AST-2241526 and Co-

operative Support Agreements AST-1202910 and AST-2211468 managed by the [Association of Universities for Research in Astronomy](#) (), and the Department of Energy under Contract No. DE-AC02-76SF00515 with the SLAC National Accelerator Laboratory managed by Stanford University. Additional Rubin Observatory funding comes from private donations, grants to universities, and in-kind support from LSST-DA Institutional Members.

This work has been supported by the French National Institute of Nuclear and Particle Physics (IN2P3) through dedicated funding provided by the National Center for Scientific Research (CNRS).

This work has been supported by STFC funding for UK participation in LSST, through grant ST/Y00292X/1.

Facilities: Rubin:Simonyi (LSSTComCam), Rubin:USDAC

Software: Rubin Data Butler (Jenness et al. 2022), LSST Science Pipelines (Rubin Observatory Science Pipelines Developers 2025), LSST Feature Based Scheduler v3.0 (Yoachim et al. 2024; Naghib et al. 2019) Astropy (Astropy Collaboration et al. 2013, 2018, 2022) PIFF (Jarvis et al. 2021), GBDES (Bernstein 2022), Qserv (Wang et al. 2011; Mueller et al. 2023), Slurm, HTCondor, CVMFS, FTS3, ESNet

APPENDIX

Glossary

Association of Universities for Research in Astronomy: consortium of US institutions and international affiliates that operates world-class astronomical

observatories, AURA is the legal entity responsible for managing what it calls independent operating Centers, including LSST, under respective cooperative agreements with the National

198 Science Foundation. AURA assumes fiducial
199 responsibility for the funds provided through
200 those cooperative agreements. AURA also is the

201 legal owner of the AURA Observatory properties
202 in Chile.

203 **AURA:** Association of Universities for Research in As-
204 tronomy.

205 **DP2:** Data Preview 2.

REFERENCES

206 Astropy Collaboration, Robitaille, T. P., Tollerud, E. J.,
207 et al. 2013, *A&A*, 558, A33,
208 doi: [10.1051/0004-6361/201322068](https://doi.org/10.1051/0004-6361/201322068)
209 Astropy Collaboration, Price-Whelan, A. M., Sipőcz, B. M.,
210 et al. 2018, *AJ*, 156, 123, doi: [10.3847/1538-3881/aabc4f](https://doi.org/10.3847/1538-3881/aabc4f)
211 Astropy Collaboration, Price-Whelan, A. M., Lim, P. L.,
212 et al. 2022, *ApJ*, 935, 167, doi: [10.3847/1538-4357/ac7c74](https://doi.org/10.3847/1538-4357/ac7c74)
213 Bernstein, G. M. 2022, gbdes: DECam instrumental
214 signature fitting and processing programs, *Astrophysics*
215 *Source Code Library*, record ascl:2210.011.
216 <http://ascl.net/2210.011>
217 Jarvis, M., et al. 2021, *Mon. Not. Roy. Astron. Soc.*, 501,
218 1282, doi: [10.1093/mnras/staa3679](https://doi.org/10.1093/mnras/staa3679)
219 Jenness, T., Bosch, J. F., Salnikov, A., et al. 2022, in
220 *Society of Photo-Optical Instrumentation Engineers*
221 *(SPIE) Conference Series*, Vol. 12189, *Software and*
222 *Cyberinfrastructure for Astronomy VII*, 1218911,
223 doi: [10.1117/12.2629569](https://doi.org/10.1117/12.2629569)

224 Mueller, F., et al. 2023, in *ASP Conf. Ser.*, Vol. TBD,
225 ADASS XXXII, ed. S. Gaudet, S. Gwyn, P. Dowler,
226 D. Bohlender, & A. Hincks (San Francisco: ASP), in
227 press. <https://dmtn-243.lsst.io>
228 Naghib, E., Yoachim, P., Vanderbei, R. J., Connolly, A. J.,
229 & Jones, R. L. 2019, *The Astronomical Journal*, 157, 151,
230 doi: [10.3847/1538-3881/aafece](https://doi.org/10.3847/1538-3881/aafece)
231 Rubin Observatory Science Pipelines Developers. 2025, *The*
232 *LSST Science Pipelines Software: Optical Survey*
233 *Pipeline Reduction and Analysis Environment*, Project
234 *Science Technical Note PSTN-019*, NSF-DOE Vera C.
235 Rubin Observatory, doi: [10.71929/rubin/2570545](https://doi.org/10.71929/rubin/2570545)
236 Wang, D. L., Monkewitz, S. M., Lim, K.-T., & Becla, J.
237 2011, in *State of the Practice Reports*, SC '11 (New
238 York, NY, USA: ACM), 12:1–12:11,
239 doi: [10.1145/2063348.2063364](https://doi.org/10.1145/2063348.2063364)
240 Yoachim, P., Jones, L., Eric H. Neilsen, J., & Becker, M. R.
241 2024, *lsst/rubin_scheduler: v3.0.0*, v3.0.0, Zenodo,
242 doi: [10.5281/zenodo.13985198](https://doi.org/10.5281/zenodo.13985198)